Supplementary Information

Thulium doped LaF_3 for nanothermometry operating over 1000 nm

Erving C. Ximendes[ac†], Alexsandro F. Pereira[a†], Uéslen Rocha[a], Wagner F. Silva[a], Daniel Jaque[bc], and Carlos Jacinto [a*]

[a] *Group of Nano-Photonics and Imaging, Instituto de Física, Universidade Federal de Alagoas, 57072-900, Maceió-AL, Brazil*
[b] *Fluorescence Imaging Group, Departamento de Física de materiales, C-04, Universidad Autónoma de Madrid, 28049, Madrid, Spain.*
[c] *Nanobiology Group, FIRYCIS Hospital Ramon y Cajal, CR. Colmenar, Km 9100, 28034, Madrid, Spain.*

[*] *E-mail: cjacinto@fis.ufal.br*
[†] *These authors contributed equally to this work.*

Figure S1 exhibits the simplified energy level diagram for the Tm^{3+} doped LaF_3 system under excitation at 790 and 690 nm. When the excitation is at 790 nm the Tm ions emit principal and basically at around 1470 nm, while under excitation at 690 arises also the emission at around 1230 nm because of the cross-relaxation processes labelled as $\gamma_{CR,2}$ and $\gamma_{CR,3}$, however the main them responsible is the first one that is almost resonant. The almost zero emission at the transition $^3H_5 \rightarrow {}^3H_6$ indicates that the cross-relaxation $\gamma_{CR,1}$ is negligible.

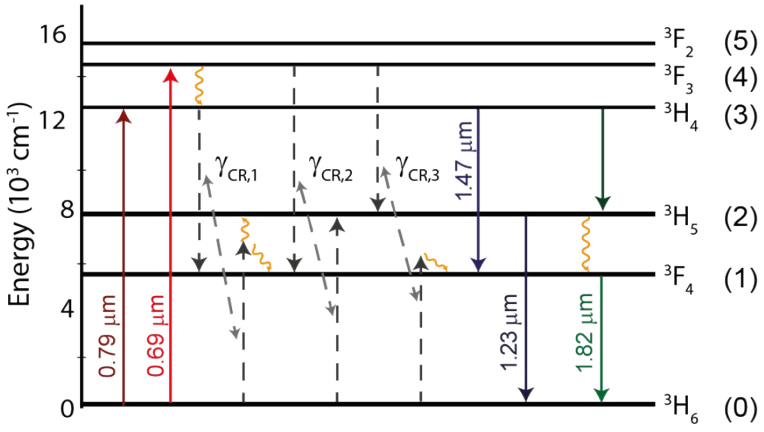

Figure S1. Simplified energy level diagram for $Tm:LaF_3$ system under excitation at 790 or 690 nm.

Figure S2 shows emission spectra of the sodium niobate ($NaNbO_3$) nanocrystals doped with 1, 3, and 5 mol% of Tm^{3+} under excitation at 690 nm. The $NaNbO_3$ is a very

interesting host for rare-earth ions as demonstrated previously [1–5], its phonon energy is of 650 cm^{-1} [5], however, under excitation at 690 nm it does not present emission at 1230 nm of the Tm ions and probably this is due to the relatively high phonon energy of this matrix favoring the multiphonon decay in the $^3H_5 \rightarrow {}^3F_4$ transition.

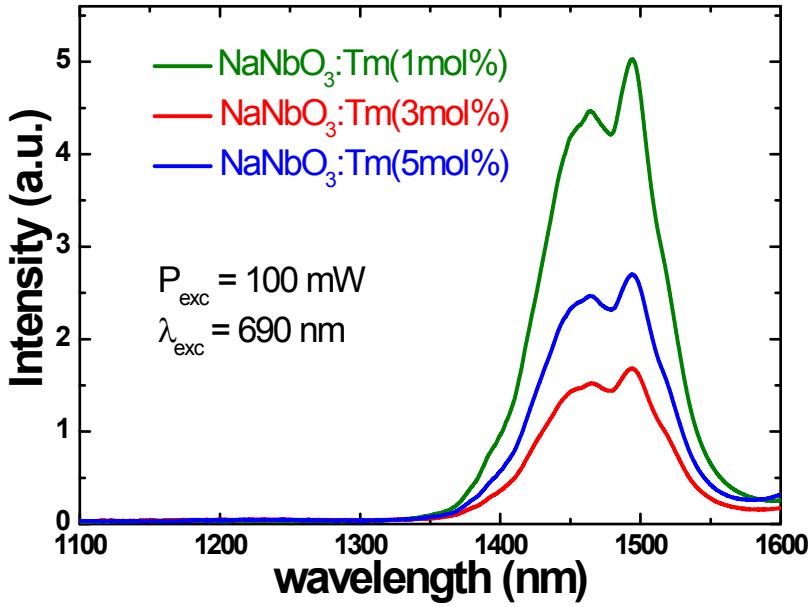

Figure S2. Near infrared (1100 – 1600 nm) emission spectra for the three $NaNbO_3$ (sodium niobate) samples doped with 1, 3, and 5 mol% under excitation at 690 nm, all with 100 mW of pump power and at room temperature.

Synthesis of the sodium niobate nanocrystals: Thulium doped single-phase $NaNbO_3$ nanocrystals ($Na_{(1-0.01\cdot x)}Tm_{(0.01\cdot x)}NbO_3$ where x = 1, 3 and 5, hereafter $NaNbO_3$:xTm NPs) were synthesized by the Pechini sol–gel method, as described elsewhere.[6] Briefly, about 19.2 g of citric acid (Aldrich, 99.5%) was added to 10 ml of water under stirring and heating at 75°C. After dissolution, 0.1836 g of ammonium niobium oxalate was dissolved and then stoichiometric quantities of Na_2CO_3 (Aldrich, 99.9%), and $Tm(NO_3)_3 \cdot H_2O$ (Aldrich, 99.99%) were added to the above transparent solution. Finally, 5.6 ml of ethylene glycol (Aldrich, > 99%) was added to the solution under regular stirring for 1 h at 75°C and then the reaction mixture was cooled to room temperature. A gel was obtained after a heat treatment at 90°C for 3 days. The gel was first heated at 400°C for 2 h, where the carbaneous precursor was formed and then a white fluffy powder was obtained at 800°C, which was the heat treatment temperature for 3 h. The structural and optical characterizations of this host can be find elsewhere.[6-7]

The set of rate equations describing the system depicted in Figure S1 for excitation at 690 nm is expressed in Equations 1-10:

$$\dot{n}_4 = R_p n_0 - \frac{n_4}{\tau_4} \tag{1}$$

$$\dot{n}_3 = W_{mp}^{43} n_4 - \frac{n_3}{\tau_3} \tag{2}$$

$$\dot{n}_2 = n_3 W_{rad}^{32} + n_4 W_{CR}^{4} - \frac{n_2}{\tau_2} \tag{3}$$

$$\dot{n}_1 = n_3 W_{rad}^{31} + n_4 W_{CR}^{4} + 2n_3 W_{CR}^{3} - \frac{n_1}{\tau_1} \tag{4}$$

where $\tau_4^{-1} = W_{rad}^{4} + W_{mp}^{43} + W_{CR}^{4}$, $\tau_3^{-1} = W_{rad}^{3} + W_{mp}^{32} + W_{CR}^{3}$, $\tau_2^{-1} = W_{rad}^{2} + W_{mp}^{21}$, $\tau_1^{-1} = W_{rad}^{1} + W_{mp}^{10}$, $W_{CR}^{4} = n_0(\gamma_{CR,2} + \gamma_{CR,3})$, and $W_{CR}^{3} = n_0\gamma_{CR,1}$. R_p is the pumping rate, n_i and τ_i are respectively the population and lifetime of the level-i, W_{mp}^{ji} and W_{rad}^{ji} are respectively the multiphonon and radiative decay rates for the $j \rightarrow i$ transition, and W_{CR}^{i} are the CR rates as indicated in **Figure S1**. The steady-state solution results in:

$$n_3 = R_p n_0 \tau_3 \tau_4 W_{mp}^{43} \tag{5}$$

$$n_2 = R_p n_0 \tau_2 \tau_4 (W_{rad}^{32} W_{mp}^{43} \tau_3 + W_{CR}^{4}) \tag{6}$$

for the two levels emitting at around 1.47 and 1.23 μm, respectively. Thus,

$$\frac{n_3}{n_2} = \frac{\tau_3 W_{mp}^{43}}{\tau_2 (W_{rad}^{32} W_{mp}^{43} \tau_3 + W_{CR}^{4})} \tag{7}$$

As the emission intensity of a specific transition is given by $I_{ji} = h\nu_{ji} W_{rad}^{ji} n_i$, where $h\nu_{ji}$ is the energy of the transition i→j and since $W_{rad}^{32} \approx 0$, we have:

$$\Delta = \left(\frac{\nu_{32} W_{rad}^{32}}{\nu_{20} W_{rad}^{20}}\right)\frac{n_3}{n_2} = \left(\frac{\nu_{32} W_{rad}^{32}}{\nu_{20} W_{rad}^{20}}\right)\frac{\tau_3 W_{mp}^{43}}{\tau_2 W_{CR}^{4}} \tag{8}$$

$n_0\gamma_{CR,2}$ and $n_0\gamma_{CR,3}$ are almost resonant and weakly temperature dependent. Similarly τ_3 is weakly temperature dependent due to the large energy gap ($W_{mp}^{32} \approx 0$ – see Figure

S3) and the CR almost resonant ($W_{CR}^{3} \approx 0$ in comparison with W_{CR}^{4}). On the other hand, W_{mp}^{21} as well as W_{mp}^{43} are strongly dependent on the temperature. Therefore:

$$\Delta(T) = A\frac{W_{mp}^{43}}{\tau_2} \tag{9}$$

$$\Delta(T) \propto \left(W_{rad}^{2} + W_{mp}^{21}\right)W_{mp}^{43} \tag{10}$$

in which $A = \frac{\nu_{32} W_{rad}^{32}\ \tau_3}{\nu_{20} W_{rad}^{20} W_{CR}^{4}}$ should be temperature independent.

The multiphonon decay follows an exponential gap law given by [8]:

$$W_{mp}^{ij}(T) = Ce^{-\alpha\Delta E}\left[1 - \exp\left(-\frac{\hbar\omega_p}{kT}\right)\right]^{-p} \tag{11}$$

in which $\alpha = -ln\varepsilon/\hbar\omega_p$, where ε accounts for the exact nature of the ion-phonon coulpling and is insensitive as the log dependence in the formula, C is a constant dependent on the phonon density of the matrix. For LaF_3 host, $C = 6.6 \times 10^8 s^{-1}$, $\alpha = -5.6 \times 10^5 cm$, $\hbar\omega_p = 350\ cm^{-1}$, $\Delta E = 2635\ cm^{-1}$ and $\Delta E = 1640\ cm^{-1}$ for $^3H_5 \rightarrow {}^3F_4$ (21) and $^3F_3 \rightarrow {}^3H_4$ (43) transitions, respectively. Figure S3 presents the multiphonons decay rates for the transitions $^3H_4 \rightarrow {}^3H_5$, $^3H_5 \rightarrow {}^3F_4$, and $^3F_3 \rightarrow {}^3H_4$.

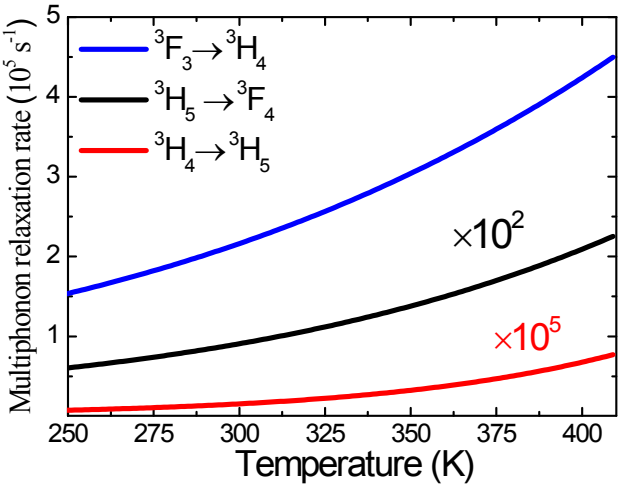

Figure S3. Temperature dependence of the multiphonon relaxation rate for the transitions $^3H_4$ → $^3H_5$, $^3H_5$ → $^3F_4$, and $^3F_3$→ $^3H_4$ with the corresponding energy gaps $\Delta E = 4370\ cm^{-1}$ (red line), $\Delta E = 2635\ cm^{-1}$ (black line), and $\Delta E = 1640\ cm^{-1}$ (blue line) for the Tm^{3+} doped LaF_3 sample.

Figure S4 presents only for instruction, the experimental data of the sample LaF_3:3Tm and the simulation using Equation (10) with $W_{rad}^{2} = 10^3 s^{-1}$ (left graph) for the normalized ratio (Δ) against the temperature. This comparison is only an attempt to validate our argument of the main temperature-dependent rates (multiphonon decays) contributing to the intensity ratio behavior. It is important to mention, however, that other processes, such as energy transfer via cross relaxation, must also contribute, even if weakly.

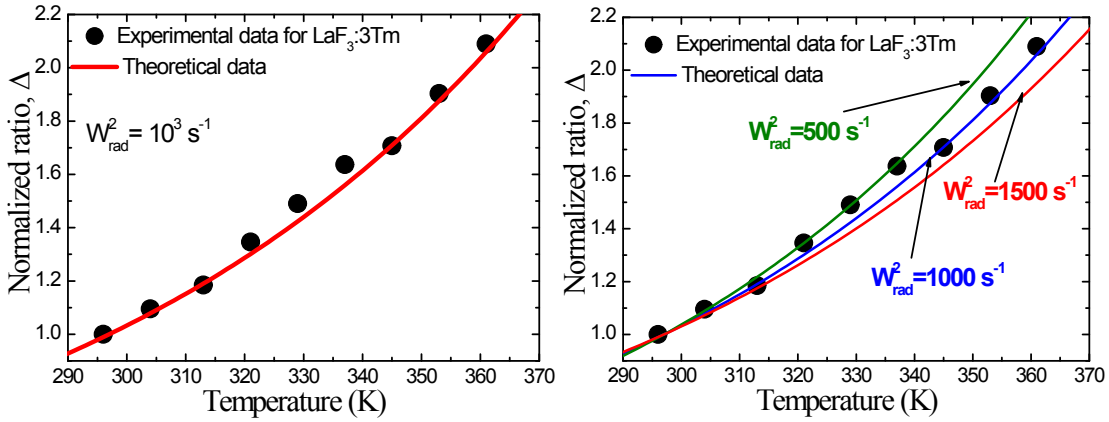

Figure S4. Temperature dependence of the normalized ratio. (Symbol) are experimental data of the LaF_3:3Tm sample and (solid line) the theoretical simulation using Equations (10) and (11) with –Left: $W_{rad}^{2} = 10^3 s^{-1}$ and -Right: $W_{rad}^{2} = 500 s^{-1}$ (green line), $W_{rad}^{2} = 10^3 s^{-1}$ (blue line), and $W_{rad}^{2} = 1500 s^{-1}$ (red line).

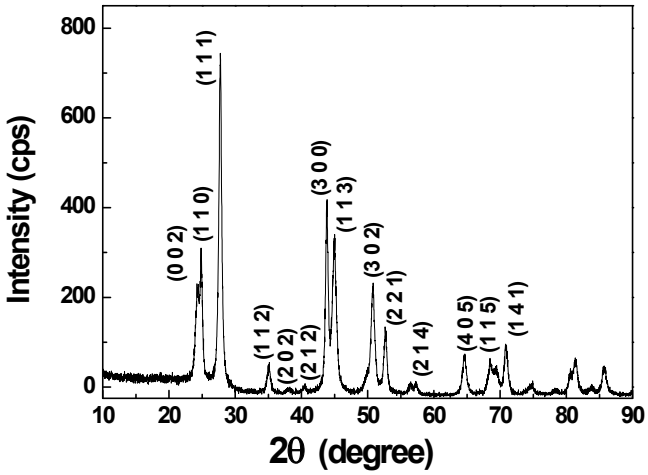

Figure S5. XRD spectrum of Tm doped LaF_3 nanoparticles used along this work and that denotes the existence of a pure hexagonal phase of LaF_3.

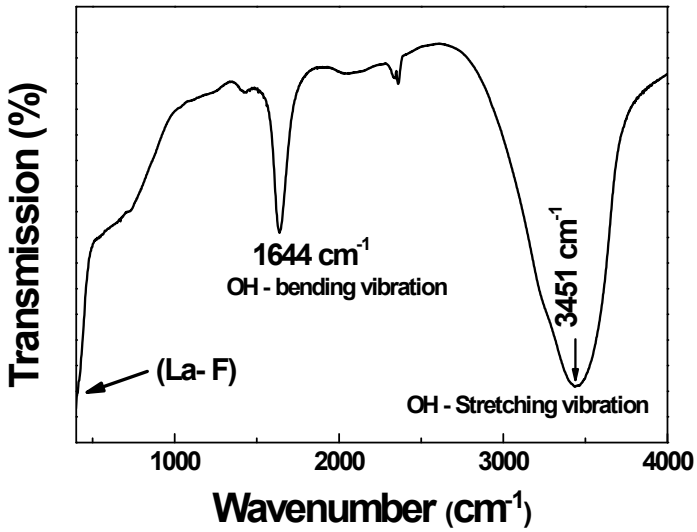

Figure S6. FTIR spectrum of Thulium doped LaF_3 nanoparticles.

Figure S7. (a) Optical image of a cuvette containing the solution used for the *ex vivo* experiment described in the main text. (b) Optical image superimposed to the fluorescence image obtained after focusing a 690 nm cw diode laser into the solution and placing a long-pass filter (1050 nm) before the IR camera.

References

1 A. F. Pereira, K. U. Kumar, W. F. Silva, W. Q. Santos, D. Jaque and C. Jacinto, *Sens. Actuators B Chem.*, 2015, **213**, 65–71.

2 A. F. Pereira, J. F. Silva, A. S. Gouveia-Neto and C. Jacinto, *Sens. Actuators B Chem.*, 2017, **238**, 525–531.

3 K. U. Kumar, W. F. Silva, K. Venkata Krishnaiah, C. K. Jayasankar and C. Jacinto, *J. Nanophotonics*, 2014, **8**, 083093.

4 K. U. Kumar, W. Q. Santos, W. F. Silva and C. Jacinto, *J. Nanosci. Nanotechnol.*, 2013, **13**, 6841–6845.

5 K. U. Kumar, N. Vijaya, J. Oliva, C. Jacinto, E. de La Rosa and C. K. Jayasankar, *Mater. Express*, 2012, **2**, 294–302.

6 K.U. Kumar, K. Linganna, S.S. Babu, F. Piccinelli, A. Speghini, M. Giarola, G. Mariotto and C.K. Jayasankar, *Sci. Adv. Mater.*, 2012, **4**, 584-590.

7 S. Pin, F. Piccinelli, K.U. Kumar, S. Enzo, P. Ghigna, C. Cannas, A. Musinu, G. Mariotto, M. Bettinelli and A. Speghini, *J. Solid State Chem.*, 2012, **196**, 1-10

8 C. B. Layne, W. H. Lowdermilk and M. J. Weber, *Phys. Rev. B*, 1977, **16**, 10–20.